Effect of astaxanthin concentration on the wear properties of castor oil and wear rate prediction using non-linear regression by pin-on-disk tests

S. Rojas-Osorio, M.U. Negrete-Ríos, M.T. Hernández-Sierra, K.J. Moreno

Numerous studies have aimed to identify biodegradable oils and additives as alternatives to mineral substances in industrial settings. Among these, castor oil combined with astaxanthin, a natural antioxidant, has demonstrated exceptional results compared to other substances. Consequently, this study examined the tribological performance of five mixtures of castor oil with different astaxanthin concentrations using sliding friction tests in a pin-on-disk tribometer based on the ASTM G99-23. For this purpose, steel disks of AISI 4140 and spheres of tungsten carbide (WC) with a diameter of 3 mm were used as counterparts. Each essay was performed by immersing the test specimens in the lubricant, controlling the temperature at 100 °C. The key finding is that the reduction in wear rate is directly affected by increasing astaxanthin concentration, which was observed in the wear mechanism. The correlation between wear rate and astaxanthin concentration was studied through a mathematical equation that estimates the value of the wear parameter at antioxidant concentrations beyond those tested experimentally. This achievement marks a significant milestone in applying statistics to complex systems, establishing a mathematical link between astaxanthin concentrations and wear properties.

Introduction

The origin of lubricating oils dates back to the birth of ancient civilizations, where animal fats were used to move large pieces made of rock or wood from one place to another. Since the creation of the wheel, there has been a need to find substances that help make movement smoother and prevent tool wear; the first attempts at lubricants for those primitive machines were based on water and animal–vegetal greases [1]. Over time, as part of human development, the Industrial Revolution made lubricants a fundamental element in the operation of machines and tools. Organic substances were gradually replaced by mineral and synthetic compounds that improved machine performance and extended their service life, increasing the efficiency of the systems and reducing costs [2]. However, these materials cause excessive pollution to the ecosystem due to improper disposal after use. For environmental reasons, over the last two decades, there has been a lot of scientific effort focused on supporting research into the use of ecological lubricants that meet current industrial demands, evaluating organic compounds to study their properties, and the most efficient ways to improve them to match or surpass the performance of commercial lubricants [3]. Currently, a discipline that studies the relationship between lubricants and the phenomena of friction and wear is known as tribology. This field has focused in recent years on the development of environmentally friendly materials that can replace mineral or synthetic lubricants while maintaining the same level of performance and quality [4].

The use of lubricants once they reach the end of their useful life is a worrying issue: they are typically dumped in abandoned and unsupervised areas and are classified as hazardous waste due to their contents (heavy metals and some chemical derivatives resulting from their degradation at high temperatures or through contact with the work environment), making them highly harmful to health and the environment [5]. This practice remains common despite the existence of companies dedicated to the collection and disposal of these materials, which are supported by the federal government [6]. According to Nogales-Delgado *et al.* [7], the global use of lubricants directly impacts seven of the Sustainable Development Goals proposed by the United Nations: affordable and clean energy, decent work and economic growth, industry, innovation and infrastructure, responsible consumption and production, climate action, life below water, and life on land [7].

This situation has created a need to explore research areas that positively impact on the environment, manage the development and use of natural resources to help mitigate climate change, and ensure that their performance in industrial activities is adequate to meet industry demands. In this context, interest is growing in green tribology, which differs from conventional tribology by considering the environmental impact of materials within its approach, including interactions with fields such as ecological engineering, biomimetic materials, and biodegradable lubrication sources [8]. Through the study of this science, 12 standards were developed based on the 12 principles of chemistry and ecological engineering, resulting in a series of statutes that promote the use of renewable materials and resources to improve modern technologies from a tribological perspective [9].

The study of biolubricants covers topics such as raw materials, renewable sources for production, optimal formulations, compatible additives, and their performance in tribological systems that simulate working conditions in laboratories [3]. In this point, the pin-on-disk method has been widely used to study the tribological effect of

S. Rojas-Osorio, M.U. Negrete-Ríos, K.J. Moreno ✉,β
Doctoral Program in Engineering Sciences, Tecnológico Nacional de México/IT de Celaya, Celaya, Guanajuato, 38010, Mexico.
β *Department of Mechanical Engineering, Tecnológico Nacional de México/IT de Celaya, Celaya, Guanajuato, 38010, México.*

M.T. Hernández-Sierra
Automotive Systems Engineering Division, Tecnológico Nacional de México/ITS de Irapuato, Irapuato, Guanajuato, 36821, México.

Received: May 14th, 2026.
Accepted: August 14th, 2026.
Published: October 30th, 2026.
© 2026 by the authors. Creative Commons Attribution
https://doi.org/10.47566/2026_syv39_1-261001

biolubricants. For instance, Su *et al.* evaluated the effect of 1-ethyl-3-methylimidazolium dicyanamide as an additive in canola oil [10]. In the same way, the operational tribological performance of curcumin [11] and deep eutectic solvents [12] have been explored as additives in castor oil under the ball-on-disk configuration.

Vegetable oils are among the most commonly used substances for producing biolubricants because, with the right combination of additives, their performance can be comparable to that of mineral lubricants and can enhance tribological properties [2,13].

Castor oil (Ricinus communis, CO) is a plant adaptable to many climates worldwide; its seeds contain approximately 45–60% oil, with ricinolein acid as the main component, which accounts for its high specific gravity, viscosity, and hydroxyl value [14]. Studies support the use of CO as a biolubricant with natural and synthetic additives, most of which focus on reducing the coefficient of friction or the wear rate of materials [14,15]. One additive that can improve the poor thermal and oxidative stability of CO is a group of natural antioxidant compounds called carotenoids, produced by bacteria, algae, plants, and fungi, exhibiting a vibrant color spectrum from yellow to red; if a molecule contains oxygen in its chemical structure (such as a hydroxyl, methoxy, or other functional group), it is classified as a xanthophyll [16]. Xanthophylls include pigments such as zeaxanthin, lutein, cryptoxanthin, fucoxanthin, and astaxanthin; astaxanthin has shown a better antioxidant performance than the other xanthophylls due to the two terminal carbonyl groups conjugated to the polyene structure; depending on the source, this compound can be synthesized from other xanthophylls [10]. Astaxanthin is an interesting topic due to its significant potential to replace synthetic antioxidants because its molecular activity in oil exceeds that of similar compounds [17]. Although the main application of astaxanthin is in the food industry, recent studies have explored ways to leverage the properties of the molecule in engineering, such as an additive for biolubricants, demonstrating good tribological performance [18,19]. In a study reported by Moreno *et al.* [16], three xanthophylls were evaluated as potential additives in green lubricants, and astaxanthin was found to perform best in terms of wear reduction. By using sliding friction tests under boundary lubrication conditions in a tribometer with pin-on-disk configuration it was found that all xanthophylls produced a slight increase in the friction coefficient of pure castor oil (μ_k = 0.095), they significantly reduced the wear rate, with astaxanthin achieving a decrease from 1.75×10^{-5} to 1.1×10^{-5} mm^3/Nm, corresponding to an improvement of ≈37% [16].

On the other hand, statistical techniques have become increasingly important in tribological science [20-22]. Researchers such as Bang *et al.* [21] have used these methods to develop effective simulation techniques for predicting quantitative wear on stamping tools. In 2024, F.O. Kolawole and S.K. Kolawole [22] studied statistical models to predict the coefficient of friction and wear for two different coatings using ANOVA and regression analysis, achieving a reliability of 90-97% in their results. This information highlights how statistical methods can help explain phenomena in tribological performance, making it essential to define the scope of the resulting equations.

For all the above, the present work focuses on deepening the analysis of how different concentrations of astaxanthin affect the wear properties of castor oil. Five different concentrations were used to prepare the biolubricants. To achieve this, a sliding contact system was performed using AISI 4140 annealed steel against tungsten carbide (WC) in a ball-on-disk configuration. To extend the understanding of higher astaxanthin concentrations, a nonlinear regression technique was employed to predict the wear behavior of AISI 4140 annealed steel.

Experimental details

Materials

The AISI 4140 annealed steel samples, measuring 25.4 mm in diameter and 5 mm in thickness, were used as disks. All samples were prepared using a standardized metallographic process with a Struers LaboPol-1 (Ballerup, Denmark) grinder until a surface roughness of 0.03 μm in Ra was achieved, as specified in ASTM G99-23 for tribological tests on a pin-on-disk tribometer [23]. The counterparts were tungsten carbide (WC) spheres of 3 mm in diameter and the same surface roughness as the disk samples. They were used in the as-received condition employing a new pin for each test. Table 1 summarizes the chemical composition and some mechanical properties of the AISI 4140 steel and WC balls. All lubricants were based on neat nonedible castor oil (CO), purchased from Abreiko (Jalisco, Mexico). Astaxanthin (CAS No. 7542-45-2) was obtained from Sigma-Aldrich.

Five lubricants were prepared with different astaxanthin concentrations in weight percent: 0.01%, 0.03%, 0.04%, 0.07%, and 0.42% (the IDs for lubricants are CA01, CA02, CA03, CA04, and CA05, respectively). These concentrations were selected based on the previous studies of the natural antioxidants as lubricant additives [16,24]. The additive powder was mixed into the oil to make 60 ml of homogeneous biolubricant by magnetic stirring in a 100 ml borosilicate beaker at 80 °C for one hour.

Physical characterization of lubricants

To understand the effect of astaxanthin concentration on the physical properties of lubricants, the kinematic viscosity was measured at 40 °C and 100 °C using Cannon Instrument glass capillary viscometers (State College, PA, USA) with a thermal bath to control the sample temperature. The viscosity index was also calculated from the viscosity values obtained from the biolubricants, according to ASTM D 2270 [25].

Tribological tests

All lubricants were evaluated in tribological tests performed at a mean contact pressure of 0.90 GPa, a temperature of 100 °C, and a sliding speed of 0.025 m/s for 30,000 cycles in a TRB pin-on-disk tribometer (Needham, MA, USA). After preparation, the lubricants were used immediately to prevent oxidation that could affect tribological performance. The steel disk and the WC sphere

Table 1. Chemical composition and properties of testing materials.

Material	C	Si	Mn	Cr	Mo	Co	W	Fe	Vickers Hardness (HV)	Young's modulus (GPa)
AISI 4140[a]	0.40	0.30	0.90	1.00	0.20	-	-	Balance	1.9[c]	210[a]
WC[b]	1.00	-	-	-	-	6.00	93.00	-	16.8[c]	650[b]

[a] Information from supplier's technical data sheet, Aluminios Riesa (CDMX, Mexico).
[b] Information from supplier's technical data sheet, Anton Paar (Graz, Austria).
[c] Data measured in a Vickers – Knoop microhardness tester Metrotec Quality Control Instrumental (Lezo, Spain).

were completely covered by immersion in the biolubricant during the entire friction test. Each mixture was tested three times to ensure reproducibility and reliability of the results. The coefficient of friction (μ_k) and the wear analysis (wear rate K and volume loss V) were evaluated according to ASTM G 99-23 [23]. At the end of each tribology test, the average μ_k was directly obtained from the Tribox 4.5R tribometer software; the μ_k reported for each lubricant is the average of the three tests. Figure 1 shows a photograph of the configuration of the tribological test. It can be noted that in this arrangement the steel disk is firmly attached to the cup, which not only transmitted the rotational motion but also served as a reservoir for the biolubricant. The counterpart ball is mounted in a holder and pressed against the disk surface under a controlled normal load.

In the tribosystem evaluated, only the AISI 4140 steel samples exhibited significant wear; the WC sphere wear was insignificant, as can be observed in Figure A1 in Appendix A. Consequently, both the reported wear rate and the wear mechanisms correspond exclusively to the response of the steel disk. For that purpose, the wear track width measurements were obtained from micrographs of each wear track section captured at 50X magnification using a bright filter in a Carl Zeiss Axio Imager A1m metallographic microscope (Göttingen, Germany) by using Zen Software. This process was repeated until a total of 100 measurements per wear track were collected (the reported values are the average of this data). The wear mechanism was analyzed in micrographs taken at 200X magnification with a bright filter. Additionally, to deepen the analysis of the wear mechanisms, a scanning electron microscope (Quanta 3D 200i, Thermo Fisher Scientific, Waltham, MA, USA) equipped with an energy-dispersive X-ray spectroscopy (EDX) accessory (Oxford X-MaxN-50, Abingdon-on-Thames, Oxfordshire, UK) was employed to characterize the surface damage. This combined approach allowed both morphological and compositional evaluation of the worn regions, providing complementary evidence to identify the dominant wear processes.

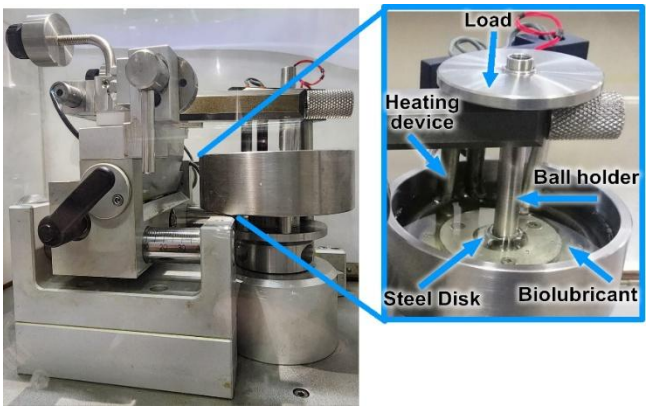

Figure 1. Photograph of tribological test configuration.

To determine the wear rate (K), Equation 1 was used

$$K = V/F \cdot S \quad (1)$$

according to the pin-on-disk method established in [23], where V represents the volume loss, F the normal load, and S the total sliding distance of the test. While the volume loss was determined by the width of wear track according to [23].

Chemical characterization of lubricants

The studied lubricants were characterized by attenuated total reflectance Fourier transform infrared spectroscopy (ATR-FTIR) before and after tribological tests. Measurements were performed using a Spectrum 100 spectrometer Perkin Elmer (Waltham, MA, USA) equipped with a $LiTaO_3$ detector, a KBr beam splitter, and an attenuated total reflectance accessory with a ZnSe crystal. Spectra were recorded in the 650–4000 cm^{-1} range, with a resolution of 4.0 cm^{-1} and an average of four scans per sample. Before and after each analysis, the ATR was thoroughly cleaned with hexane, and a background spectrum was acquired to eliminate potential environmental interference.

Wear rate estimation using a non-linear regression model

Non-linear regression analysis is recommended when the relationship between input and output variables does not follow a proportional increase or decrease, as is typical in most tribological systems. In this study, the focus is on estimating wear rate (K) using astaxanthin concentration (wt%) as the input variable. The analysis extends the concentration range to explore the effects if the additive reaches 2% in the biolubricant. Based on this approach, K and five different astaxanthin concentrations were used for linear and non-linear regression analysis, evaluating the coefficient of determination (R^2). This coefficient is commonly described as the percentage of variation of the dependent variable (wear rate) explained by the variation in the independent variable (astaxanthin concentration) [26]. Selecting the best fit ($R^2 \approx 1$), resulting in a power equation that follows the trend of the experimental data [26].

© Sociedad Mexicana de Ciencia y Tecnología de Superficies y Materiales

Table 2. Kinematic viscosity and viscosity index of lubricants.

Lubricant	Kinematic viscosity (mm^2/s)		Viscosity index, VI
	40 °C	100 °C	
CO	265	22	99.97
CSA01	263	21.7	98.92
CSA02	254	21.5	100.83
CSA03	250	21.4	101.76
CSA04	231	21.3	109.67
CSA05	223	18.4	90.82

Results and discussion

Physical characterization of lubricants

Table 2 shows the kinematic viscosity and viscosity index of the biolubricants. The results show that the concentration of astaxanthin in castor oil influences these properties. Kinematic viscosity at 40 °C decreases progressively as the concentration increases, suggesting that the presence of the additive facilitates molecular mobility and reduces the fluid's internal resistance. This behavior is particularly pronounced starting at CA04, where the viscosity drop is significant compared to the base oil. In contrast, the viscosity index (VI) reveals a non-linear trend: it remains close to 100 at low concentrations, reaches a maximum at CA04 (VI = 109.67), indicating an improvement in the lubricant's thermal stability, and then drops sharply to 90.82 at CA05.

Tribological results

The average μ_k for each lubricant is shown in Figure 2a. It can be noted that increasing or decreasing the astaxanthin concentration does not appear to affect this variable. The highest μ_k corresponds to CA03 (which is not the lubricant with the most additive), while the lowest value corresponds to the lowest astaxanthin concentration. This behavior varies depending on the additive; its chemical composition, concentration, and dispersion influence the friction properties of the lubricant in different ways. Some researchers have observed that optimal frictional performance occurs at the lowest additive concentrations [16,19,27]. For example, Liñeira del Río reported that the greatest reduction was achieved with a low concentration of 0.1 wt% of deep eutectic solvent (DES1) as an additive in castor oil [12]. Interestingly, in that study, the friction coefficient values were 30% higher at the same additive mass concentration as in the present study. Figure 2b shows the friction coefficient behavior of each mixture as a function of cycles. It can be observed that CA01 starts with low values and remains stable around 0.1, showing minimal fluctuations and rapid stabilization. CA02 presents slight initial variations but converges towards an intermediate range close to 0.12, with a tendency to stabilize after 15×10^3 cycles. CA03 exhibits the highest values, with a progressive increase to approximately 0.15, while CA04 is in the medium-high zone, with moderate oscillations and stabilization towards 0.11–0.12 after 20×10^3 cycles. CA05 shows more marked fluctuations in the first cycles reaching up to 0.135 but finally converges around 0.10–0.11. Overall, it is observed that the lubricants tend to stabilize after a certain number of cycles, with clear differences in the level of friction achieved.

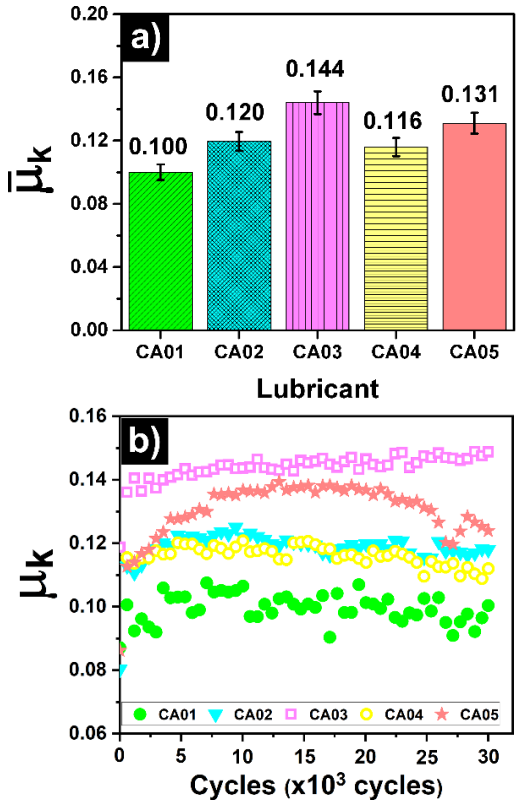

Figure 2. Friction coefficient for biolubricants with different concentrations of astaxanthin: a) average values and b) behavior of individual tests.

Regarding the wear analysis, Figure 3 depicts the relationship between the wear track width (WTW) and wear rate (K) for each biolubricant, while Table 3 summarizes the corresponding volume loss (V). One of the first characteristics evaluated was the WTW, which showed a decreasing trend as the concentration of astaxanthin increased. Consistently, both the wear rate and the volume loss followed the same downward tendency, highlighting the positive influence of astaxanthin on the tribological performance of the biolubricants. It is important to note that although the main purpose of adding astaxanthin as an additive was to protect the oil from oxidation during operation, this action also benefits surface interactions by reducing the wear rate of the involved materials. Several investigations in green lubricants have been reported that some primary antioxidant additives such as propyl gallate [27], curcumin, eugenol, 1,3-Diphenyl-2-propanone, 1,3-Diphenyl-2-propenone, and 1,3-Diphenyl-1,3-propanedione [24] have also provided effective surface protection characterized by low wear rate values, despite higher friction coefficients [24,27].

Table 3. Volume loss V for each biolubricant.

Lubricant	CSA01	CSA02	CSA03	CSA04	CSA05
V ($\times10^{-3}$ mm^3)	8.61	4.79	4.35	4.00	2.00

© Sociedad Mexicana de Ciencia y Tecnología de Superficies y Materiales

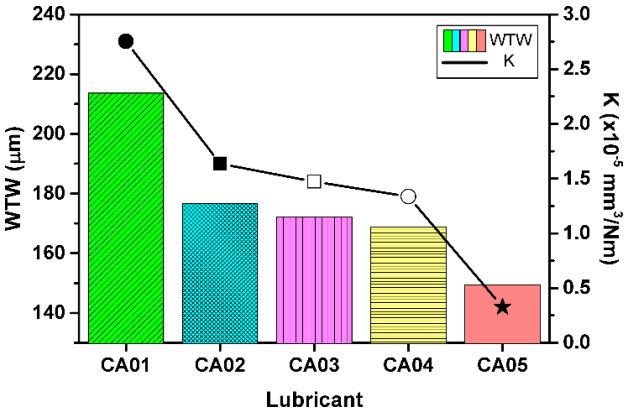

Figure 3. Wear track width (WTW) and wear rate (K) obtained with each lubricant.

The wear mechanism on the surface of AISI 4140 steel for each biolubricant with different astaxanthin concentrations is shown in Figure 4, which displays the wear track profile and a 2.5D image of the surface track. The main wear mechanism observed is abrasion at all concentrations, with characteristic grooves associated to this mechanism [28], running parallel to the sliding contact and visible on all surfaces. As astaxanthin concentration increases, adhesion signs become more pronounced, especially in samples CA03 and CA05. A change in the wear mechanism due to increased antioxidant concentration was reported by Keno *et al*. [27], who evaluated the performance of castor oil as a biolubricant for agricultural tractor engines, with concentrations ranging from 0.25 v% to 2 v% of a mixture of propyl gallate and ionic liquid as additives. These tests found that antioxidant concentration influenced wear behavior, resulting in a smoother wear track with adhesive and abrasive zones. Unlike the experiments of Keno *et al*., which showed a negative response in the metallic system as the additive concentration increased, the present work shows a direct, positive relationship between wear reduction and the highest astaxanthin concentration.

Figure 5 presents the SEM and EDX analyses of the wear surface of AISI 4140 steel lubricated with CA04, as a representative case. The SEM micrograph clearly reveals an abrasive wear mechanism, evidenced by the presence of pronounced groove marks aligned with the sliding direction. This morphological feature confirms that the dominant wear process was governed by abrasive particles or asperities. Complementary EDX spectra provides chemical insight into the worn regions, supporting the interpretation of the prevailing wear mode. These analyses were performed in two specific regions: one within a wear groove (Spectrum 317) and the other on the worn surface (Spectrum 318). In the first case, in addition to the characteristic elements of steel, a significant fraction of oxygen was detected. This finding suggests the occurrence of an oxidation wear mechanism, whose products remained trapped within the grooves. In contrast, the second analysis primarily revealed the constituent elements of steel, indicating that in that area the deterioration process was dominated by physical mechanisms associated with contact and mechanical material removal.

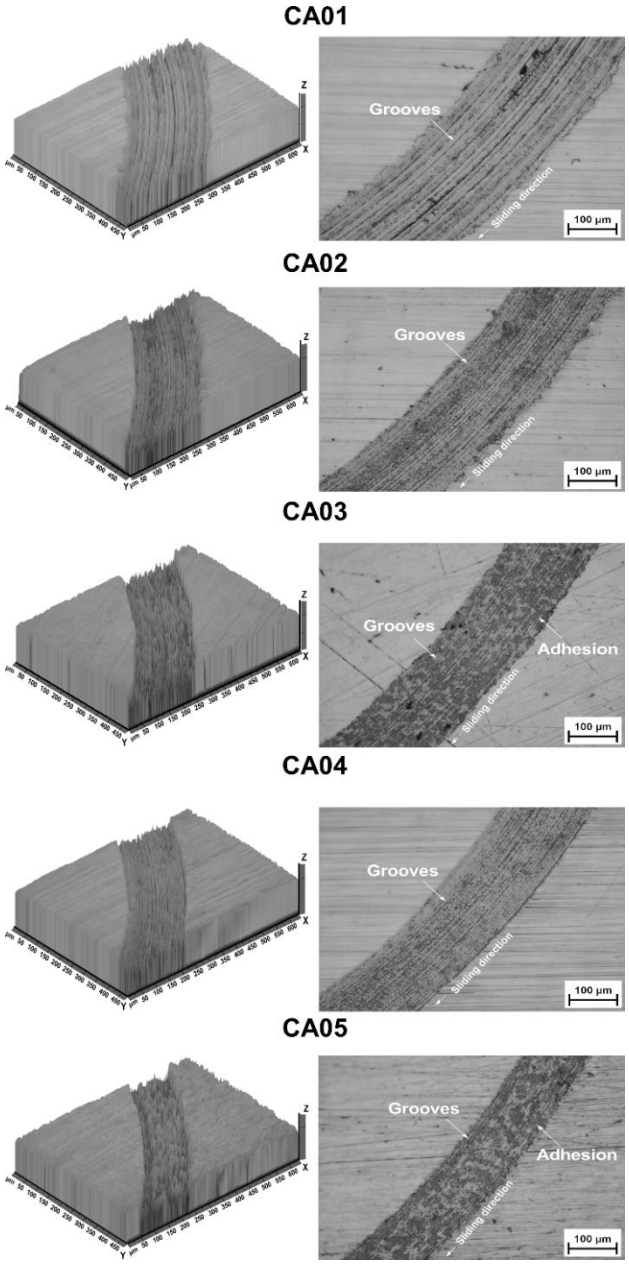

Figure 4. Wear track roughness profile at 2.5D image and the wear surface mechanism of biolubricants.

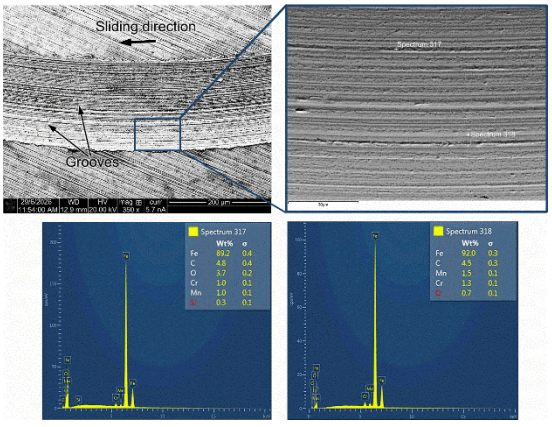

Figure 5. SEM and EDX analysis on the wear surface lubricated with CA04.

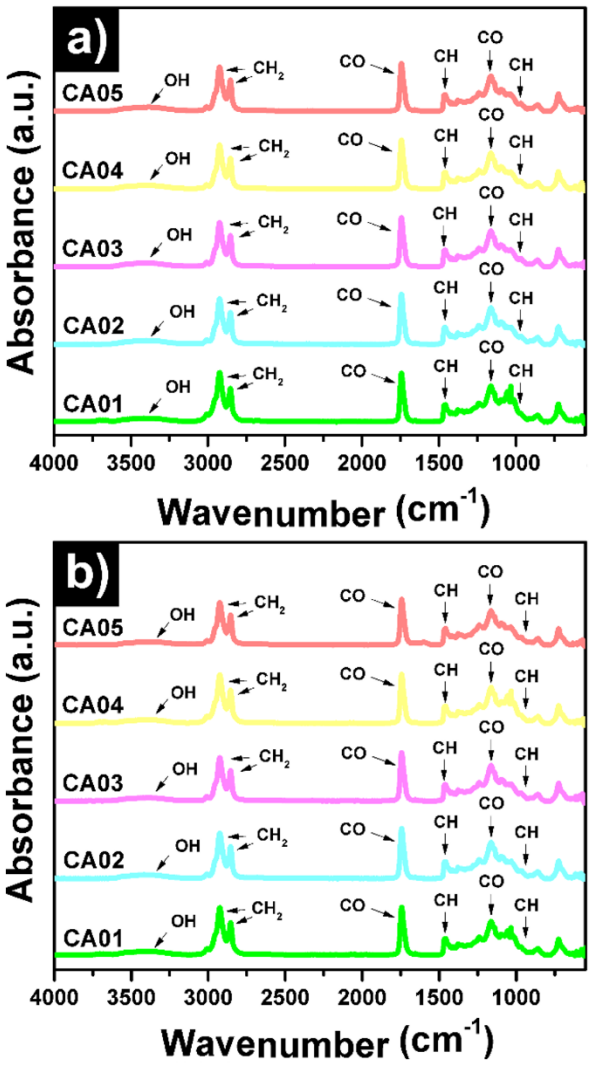

Figure 6. FTIR spectra of lubricants: a) before and b) after tribological tests.

Chemical characterization of lubricants

The ATR-FTIR spectra of the lubricants recorded before and after the tribological tests are presented in Figure 6. As shown in Figure 6a, the spectral features correspond to the base oil, and the presence of the additive does not significantly modify either the intensity or the position of the characteristic absorption bands. The broad band centered at approximately 3430 cm^{-1} is attributed to the stretching vibrations of the hydroxyl (O–H) group, a distinctive feature of castor oil. The strong absorptions at around 2924 cm^{-1} and 2855 cm^{-1} arise from the asymmetric and symmetric stretching vibrations of methylene (CH_2) groups, respectively. The intense band observed near 1743 cm^{-1} corresponds to the ester carbonyl (C=O) stretching vibration, confirming the triglyceride structure of the oil. Additional signals between 1500 and 650 cm^{-1} define the fingerprint region typical of vegetable oils, where the peaks at 1460 cm^{-1} and 1370 cm^{-1} are associated with the symmetric bending vibrations of CH_2 and CH_3 groups [11,26].

On the other hand, Figure 6b demonstrates that tribological tests do not induce substantial alterations in the overall spectral profile. To further investigate potential oxidative changes, the integrated area of the carbonyl (C=O) band was quantified, as variations in this region are indicative of oxidation processes. The corresponding results are summarized in Table 4, providing a comparative evaluation of the oxidative stability of the lubricants under the applied testing conditions. It can be observed that CA01 exhibited a slight increase (+2.9%) in the carbonyl band area, suggesting a low degree of oxidation. In contrast, CA02, CA03, and CA04 showed negligible decreases (<1%), indicating that the tribological tests did not significantly promote oxidative degradation in these lubricants. Notably, CA05 displayed the largest reduction (–5.9%), which may be associated with structural rearrangements or consumption of carbonyl-containing species rather than oxidative progression. Overall, these findings confirm that the spectral profiles remain largely stable after tribological testing, with only slight variations in the carbonyl region. However, a more comprehensive evaluation including extended thermal and oxidative stability studies would be required to fully establish the antioxidant behavior of the additive and its long-term effectiveness in the lubricants.

Table 4. Integrated area of the carbonyl (C=O) band before and after tribological tests.

Lubricant	C=O peak Area		Change %
	Before	After	
CA01	5.54	5.70	2.91
CA02	5.70	5.68	–0.30
CA03	5.61	5.59	–0.33
CA04	5.60	5.55	–0.81
CA05	5.56	5.23	–5.89

Wear rate estimation

One of the most valuable techniques for achieving the main goal of this research is regression analysis, which involves a mathematical relationship between input and output variables, helping to identify trends and the influence between variables; this makes it easier to predict how the values will behave [29]. Figure 7 shows theoretical data calculated using linear and non-linear fits, with the experimental data for the wear rate K at the five astaxanthin concentrations as a baseline, as part of the estimation analysis to find an equation describing the behavior of K. As can be seen, even though the first four points could appear to correspond to a linear fit, the behavior of the fifth value is completely different, causing the coefficient of determination R^2 to reach a low level of 0.51. On the other hand, with the non-linear fit, the trend of the theoretical data has a better adjustment in comparison with the experimental behavior, achieving an R^2 of 0.99, which represents a significant improvement in the evaluation of the accuracy of the estimation equation. Given the R^2 value, the non-linear fit equation was chosen to estimate K's behavior.

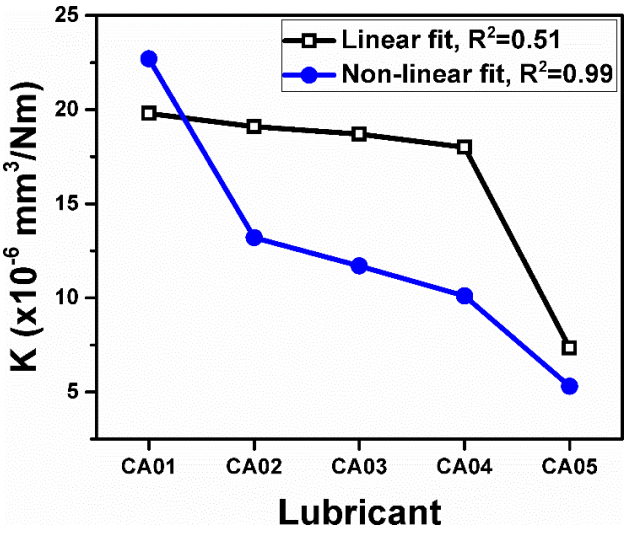

Figure 7. Linear and non-linear fits of experimental K, and R^2 values.

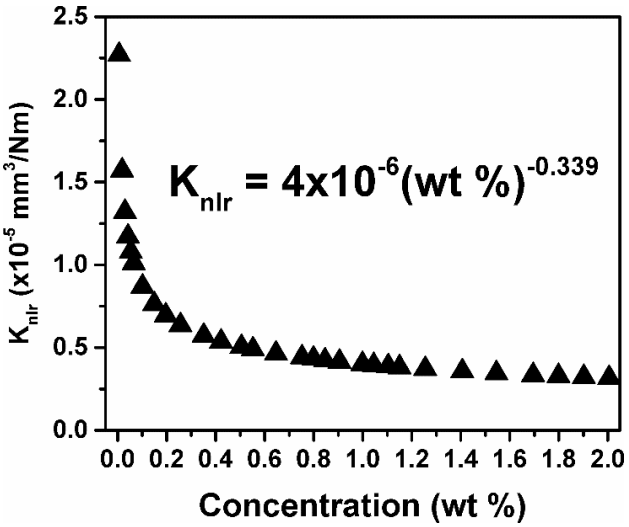

Figure 8. Theoretical wear rate values obtained using Equation 2.

Considering the above results, a non-linear regression approach was selected because it yielded the highest coefficient of determination of R^2. This coefficient is one of the most common metrics for evaluating how accurately an equation predicts values; it ranges from 0 to 1 and indicates the proportion of variance in the output variable explained by the input variable [30]. Different authors have used this method to predict tribological properties; for example, Kumar *et al.* [31] developed and analyzed a hybrid aluminum metal matrix composite from the fabrication process through material characterization, including tribological behavior. They used four different statistical models to predict the wear rate and coefficient of friction, finding that Gaussian Process Regression was the best, with an R^2 of up to 0.96. Similarly, Ativor *et al.* [32] evaluated eight models to predict the wear rate of an excavator bucket, achieving R^2 values up to 0.99 with the ICA-XGBoost model. Another example is the study by Shen *et al.* [33], in which they predicted the wear rate and estimated the remaining lifespan of a tool using two regression analyses to minimize errors [33].

In the present study, the outcome of this analysis was Equation 2, which was used to calculate the wear rate K across astaxanthin concentrations ranging from 0.01% to 2% with an $R^2 = 0.99$. In this equation, *K* will be represented as K_{nlr}, where the subscripts *nlr* stand for the initials of non-linear regression. Also, the deviation between experimental and theoretical data was calculated; this is one way to ensure the reliability of the information generated.

$$K_{nlr} = 4 \times 10^{-6}(wt\ \%)^{-0.339} \qquad (2)$$

The trend of this data is shown in Figure 8 which shows that K does not stabilize at any point; however, after 1.5 wt%, the changes in K begin to level off and exhibit a flatter trend. This may indicate the maximum astaxanthin concentration required to minimize wear rate. Additional data might be needed to explore the additive saturation capacity in biolubricant mixtures [16,24]. This information supports the development of vegetable-based lubricants with improved antioxidant properties and aids in evaluating these additives, reducing material waste and potentially shortening experimental times. To verify the accuracy of the nonlinear regression as a predictive tool, the experimental values were compared to the theoretical values from Equation 2.

Table 5 presents both experimental and theoretical data, with an absolute deviation between 0.4 and 4.7%, which is acceptable for laboratory results. The Mean Absolute Percentage Error (MAPE) provides an easy-to-understand measurement that shows the actual absolute error in relation to its average. It was used to demonstrate the accuracy of the model because it reflects the average of all differences between the data. A lower MAPE indicates higher accuracy; 0% represents a perfect fit. In this case, the MAPE is less than 2.5%, suggesting the equation can predict with high accuracy [34,35].

According to the results shown in Table 5, the equation describes K as a non-linear function. It can be extrapolated if the test conditions are maintained and if the astaxanthin concentration is higher or lower. The statistical approach in this type of study is a strategy for simulating the behavior of a complex system using a simple mathematical relationship, focusing on a parameter of interest. There are many techniques for analyzing, and the chosen one depends on the nature of the phenomenon being studied.

It is important to emphasize that the present work aims to establish a baseline for applying analytical models and simplified equations to describe complex phenomena, such

Table 5. Comparison between K and K_{nlr}, differences for each lubricant, and MAPE.

Lubricant	K	K_{nlr}	Absolute deviation (%)	MAPE (%)
	($\times 10^{-5}$ mm³/Nm)			
CSA01	2.28	2.27	0.4	
CSA02	1.27	1.32	3.9	
CSA03	1.15	1.17	1.7	2.45
CSA04	1.06	1.01	4.7	
CSA05	0.53	0.54	1.1	

as wear rate, while offering valuable insight into the overall behavior of the system. Building upon this foundation, future research will involve conducting additional experiments with a wider range of astaxanthin concentrations to further validate and expand the scope of the findings.

Conclusions

This work investigated how astaxanthin concentration influences the wear properties of castor oil used as a biolubricant in a metallic tribosystem, AISI 4140 steel/WC. It also conducted a predictive analysis of the effect of higher astaxanthin concentrations on wear rate using a non-linear regression method. The main conclusions are:

- The addition of astaxanthin to castor oil slightly reduces the kinematic viscosity with the increase in concentration. Whereas the viscosity index reaches a slight increase up to 10%, indicating greater thermal stability, but decreases at higher concentrations.
- Increasing astaxanthin concentration significantly reduces the wear rate by up to 86%.
- Astaxanthin concentration affects the worn surface, with abrasion wear being predominant at lower concentrations and adhesive wear occurring at concentrations above 0.04%.
- Stable wear rate values are achieved with concentrations of 1.5% to 2% astaxanthin.
- The incorporation of astaxanthin did not significantly alter the ATR-FTIR spectra of the neat castor oil before and after tribological tests. The characteristic absorption bands remained stable, with only slight variations observed in the carbonyl (C=O) region, suggesting certain anti-oxidative influence under the applied experimental conditions.
- The non-linear regression analysis broadens potential applications in many systems with similar vegetable oils and natural additives.

In summary, this study not only validates the improvement on wear behavior using astaxanthin as an additive but also paves the way for greener lubricants that are better suited to the demands of modern industry. Taking together, tribological testing and statistical modeling provide a solid foundation for the development of next generation of biolubricants.

Acknowledgements

The authors acknowledge Tecnológico Nacional de México (TecNM) for its support with the project CELA-PYR-2026-24486. S. Rojas-Osorio and M. U. Negrete-Ríos recognizes the Secretaría de Ciencia, Humanidades, Tecnología en Innovación (Secihti) in Mexico for the grant for doctoral studies.

References

[1]. D.V.V. Monikandan, D.K. Pratheesh, C. Santulli, S. Digra, P.V. Prasanth, E.R. Dhas, *Tribol.: Finn. J. Tribol.* **41**, 4 (2024).
[2]. E. Doğan, S. Yalçinkaya, M. Kurtulmuş, An evaluation on the principles of tribology and usage in wear applications. In: *Innovative Technology Applications in Engineering Sciences*, Eds. R. Jain, A. Güllü, S. Yalçinkaya (GÜVEN PLUS, Istanbul, 2022) pp. 74-95.
[3]. M. Khadem, W.B. Kang, D.E. Kim, *Int. J. of Precis. Eng. and Manuf.-Green Tech.* **11**, 565 (2024).
[4]. N.V. Minh, Al. Kuzharov, L.H. Ninh, N. Huynh, An. Kuzharov, Green Tribology. In: *Tribology in Materials and Manufacturing - Wear, Friction and Lubrication*, Eds. A. Patnaik, T. Singh, V. Kukshal (IntechOpen, London, 2021).
[5]. A. Acosta Valdés, J.A. Padilla Bautista, J.A. Zepeda-Domínguez, S. Ojeda-Benitez, *Rev. Int. Contam. Ambient.* **40**, 503 (2023).
[6]. Secretaría de Medio Ambiente y Recursos Naturales, Empresas autorizadas para el manejo de residuos peligrosos, *Documentos SEMARNAT* [Access: May 11th, 2026].
[7]. S. Nogales-Delgado, J.M. Encinar, J.F. González, *Catalysts* **13**, 1299 (2023).
[8]. J. Pichler, R.M. Eder, C. Besser, L. Pisarova, N. Dörr, M. Marchetti-Deschmann, M. Frauscher, *Green Chem. Lett. Rev.* **16**, 1 (2023).
[9]. M. Freschi, A. Paniz, E. Cerqueni, G. Colella, G. Dotelli, *Lubricants* **10**, 129 (2022).
[10]. Y. Su, F. Chen, J. Chen, M. Wang, *Food Sci. Hum. Wellness* **13**, 1739 (2024).
[11]. M.T. Hernández-Sierra, J.E. Báez, L.D. Aguilera-Camacho, J.S. García-Miranda, K.J. Moreno, *Proc. Inst. Mech. Eng. J: J. Eng. Tribol.* **237**, 578 (2023).
[12]. J.M. Liñeira del Río, A. Aourdou, G. García-Marquínez, J.M. Amado, M.J. Tobar, *Lubricants* **13**, 456 (2025).
[13]. D.F. Silva-Alvarez, I. Dominguez-Lopez, M.A. Vidales Hurtado, C. Gutierrez-Antonio, K.A. Flores-Garay, A.L. Garcia-Garcia, *Environ. Technol. Innov.* **33**, 103532 (2024).
[14]. T.Y. Woma, T.D. Ipilakyaa, A.A. Abdullahi, A.S. Abdulrahman, M.A. Olutoye, S.A. Lawal, *Arid Zone J. Eng. Technol. Environ.* **21**, 328 (2025).
[15]. M.M.F. Melo Neta, R.R.C. Monteiro, P.R.C.F. Ribeiro Filho, C.L. Cavalcante, F.M.T. Luna, *Lubricants* **14**, 77 (2026).
[16]. K.J. Moreno, M.T. Hernández-Sierra, J.E. Báez, E. Rodríguez-deLeón, L.D. Aguilera-Camacho, J.S. García-Miranda, *Materials* **14,** 5431 (2021).
[17]. Y. Dang, Z. Li, F. Yu, *Antioxidants* **13**, 879 (2024).
[18]. W. Hajeer, A. Blanco, A.P. Miller, J. Amengual, *Biochim. Biophys. Acta Mol. Cell Biology of Lipids* **1870**, 159619 (2025).
[19]. E. Rodríguez-deLeón, M. Bah, J.E. Báez, M.T. Hernández-Sierra, K.J. Moreno, A. Nuñez-Vilchis, J. Bonilla-Cruz, K.J. Shea, *RSC Adv.* **12**, 30851 (2022).
[20]. A. Shivaramakrishna, S. Raghavendra, Y. Basavaraj, R.A. Kumar, M.R. Kumar, N.K. Kumar, R. Suresh, *Superf. Vacío* **39**, 260301 (2026).
[21]. J. Bang, M. Kim, G. Bae, H.G. Kim, M.G. Lee, J. Song, *Materials* **15**, 4509 (2022).
[22]. F.O. Kolawole, S.K. Kolawole, *Discov. Mater.* **4**, 36 (2024).
[23]. ASTM G99-23, *Standard Test Method for Wear and Friction Testing with a Pin-on-Disk or Ball-on-Disk Apparatus* (ASTM International, 2023).
[24]. M.T. Hernández-Sierra, J.E. Báez, L.D. Aguilera-Camacho, J.S. García-Miranda, K.J. Moreno, *Lubricants* **12**, 244 (2024).
[25]. ASTM D2270-10, *Standard Practice for Calculating Viscosity Index from Kinematic Viscosity at 40 °C and 100 °C.* (ASTM International, 2016).
[26]. D. Britto Figueiredo Filho, J.A. Silva Júnior, E. Carvalho Rocha, *Leviathan (São Paulo)* **3**, 60 (2011).
[27]. W.D. Keno, Á. Kalácska, D. Fauconnier, V.R. Ancha, P. De Baets, *Lubricants* **13**, 206 (2025).
[28]. K. Kato, Classification of Wear Mechanisms/Models. In: Wear - Materials, Mechanisms and Practice. Ed. G.W. Stachowiak (Wiley, Chichester, 2005).

[29]. N.K. Kumar, R.K. Shah, S. Kumar Sahani, *Mikailalsys J. Adv. Eng. Intl.* **2** 159 (2025).
[30]. J. Gao, *Res. Methods Med. Health Sci.* **5**, 104 (2023).
[31]. P. Kumar, B. Kumar, S. Pratap, S.M.M. Hasnain, B.A. Alkhaleel, *Results Eng.* **26**, 104612 (2025).
[32]. G. Ativor, Y.Y. Ziggah, V.A. Temeng, *Ghana J. Technol.* **9**, 77 (2025).
[33]. L. Shen, B. Du, H. Fan, H. Yang, *Machines* **13**, 355 (2025).
[34]. C.D. Lewis, *Industrial and Business Forecasting Methods*, 1st ed. (Butterworth Scientific, London, 1982).
[35]. K. Warneke, S.D. Siegel, J. Afonso, S. Wallot, *Ger. J. Exerc. Sport Res.* (2025).

© 2026 by the authors; licensee SMCTSM, Mexico. This article is an open access article distributed under the terms and conditions of the Creative Commons Attribution license (http://creativecommons.org/licenses/by/4.0/).

Appendix A.

Wear of Pin Specimens

Figure A1 shows two optical micrographs of the worn surface section of the ball specimen tested with CA04 taken at 200X with a bright filter. It can be observed that after the friction test, the sphere shows no signs of material shedding. Only a surface stain is observed, attributable to material transfer from the disk that adhered to its surface.

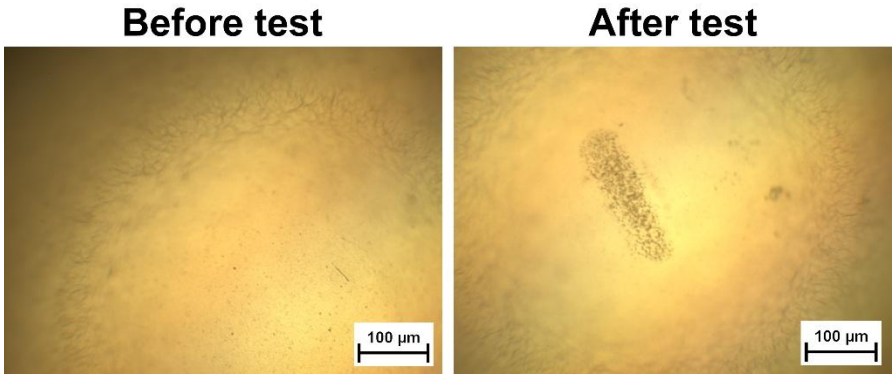

Figure A1. Worn surface of WC pin specimen tested with CA04.